

Aqueous Extract of Cumaru (*Dipteryx odorata*) Seeds as Corrosion Inhibitor for Mild Steel in Hydrochloric Acid Solution

Viviane M. Teixeira,^{ib}^a Gustavo A. de Oliveira,^a Michelle J. C. Rezende^{ib}^{*,a} and Eliane D'Elia^{ib}^a

^aInstituto de Química, Universidade Federal do Rio de Janeiro, Av. Athos da Silveira Ramos, 149, Centro de Tecnologia, Bloco A, Cidade Universitária, 21941-909 Rio de Janeiro-RJ, Brazil

The corrosion inhibition of mild steel by aqueous extract of cumaru (*Dipteryx odorata*) seeds and its high molecular weight fraction (HMWF) was investigated in 1 mol L⁻¹ HCl solution. The study was carried out through gravimetric essays, open circuit potential measurements, anodic and cathodic polarization curves and electrochemical impedance analyses, as well as morphological analysis of the mild steel by scanning electron microscopy. Gravimetric tests showed that the inhibition efficiency (IE) increased with immersion time and inhibitor concentration, reaching 98% of IE using 100 mg L⁻¹ of the HMWF, after 6 h immersion time. The activation energy (E_a) increased with the addition of both inhibitors which characterizes a physical adsorption of the constituents of the aqueous extract of cumaru on the metal surface. Polarization curves indicated that both aqueous cumaru seeds extract and its HMWF act as mixed-type inhibitor. Impedance results showed a decrease in double layer capacitance (C_{dl}) and an increase in charge transfer resistance (R_{ct}) evidencing a typically screening effect. The adsorption of molecules present in the aqueous extract of cumaru followed the Langmuir isotherm. The aqueous cumaru seeds extract was characterized by Fourier transform infrared spectroscopy (FTIR), ¹H, ¹³C and 2D nuclear magnetic resonance (NMR).

Keywords: acid corrosion, mild steel, natural inhibitor, cumaru seeds, electrochemical analyses

Introduction

Oil is the most important component of global energy and it is considered a key element for the good functioning of a country's economy. Among the challenges in the oil sector, corrosion is included. It can generate millions of dollars in losses if mismanaged, and may even affect the environment with irreparable damage. Corrosion is present in the oil industry attacking the metallic surface of tanks, pipelines and other equipments. In general, it is a spontaneous process, reducing the durability and performance of metallic materials. It is important to emphasize that the reactions that occur in the corrosive environment, in the material-corrosive environment interface, in the material and the mutual influence between them, are responsible for characteristic processes that end up causing specific or generic damages. Mild steel is an iron-carbon alloy that has up to 2% carbon and has been the most used material in the great majority of goods-producing

industries. Despite its low cost and wide use, exposure to deterioration also occurs extensively. The technology of this steel is very well developed representing an economical choice for the most diverse applications. Several alternatives have been studied¹⁻⁶ for optimal corrosion control, including the application of inhibitors.

Corrosion inhibitors are organic or inorganic compounds that, added to the corrosive medium in appropriate concentration, could reduce or prevent the reactions responsible for the corrosion.⁷ Inhibitors have been applied in acidic and neutral environments in order to protect different metals such as carbon steel, nickel and zinc. Considerable progress has been made in both manufacture of new iron alloys and development of novel materials. Adequate corrosion control is guaranteed by sum of the benefits obtained by several factors among which highlights the injection of corrosion inhibitors.⁸

The synthetic inhibitors have been widely traded for decades and the application of these substances to prevent corrosion is a success. Even so, it is known that the use of these inhibitors, mostly organic compounds containing

*e-mail: mjcrezende@gmail.com

sulfur and/or nitrogen atoms, can be highly toxic to the environment and costly.⁹⁻¹⁵ The search for environmentally friendly inhibitor is necessary, in order to reduce or completely avoid the impact on the environment. In this context, the natural inhibitors are becoming increasingly noteworthy because they come from renewable resources such as bark, seeds, leaves, fruits and often agro-industrial waste.¹⁶⁻²⁶ In Brazil, the processing of agricultural products for the extraction of juices, oils and sauces for human consumption generates a large amount of by-products from industrial treatment.¹⁶

Cumaru (*Dipteryx odorata*) is a noble wood, aromatic and medicinal tree, native to the Amazon, with different characteristics from common species. It presents high structural strength, being widely used in the timber industry.²⁷ The genus name, *Dipteryx*, comes from Greek and refers to the two wings on the leaf rachis, while the specific name, *odorata*, comes from the seed odor.²⁸ Its seeds have red wine color, but when mature they become black. They are known as tonka-beans and are used for perfumery purposes since the nineteenth century. The seeds are rich in coumarin, a phenolic compound that inhibits germination and is the main active ingredient of this plant, being responsible for much of the cumaru tree's properties.^{29,30} Specialized literature indicates that each cumaru almond has an average yield of 3% of coumarin, which can reach up to 10%.

This work investigated the inhibitory action of the aqueous extract of cumaru seeds on the corrosion of mild steel in 1 mol L⁻¹ HCl solution, using gravimetric essays, potentiodynamic polarization curves, electrochemical impedance measurements and surface analysis by scanning electron microscopy. As far as we know it is the first study that evaluated an extract of cumaru (*Dipteryx odorata*) as corrosion inhibitor.

Experimental

Solution preparation

All tests were performed with a 1 mol L⁻¹ aqueous hydrochloric acid solution prepared from 37% HCl concentrated solution (Merck Co., Darmstadt, Germany) and double-distilled water.

Obtaining the inhibitor

The seeds of cumaru (*Dipteryx odorata*) were purchased at a market in Rio de Janeiro city. About 30 g of the seeds were ground using a mini processor. These seeds were added in a beaker containing 300 mL of distilled water

previously boiled at 100 °C. The infusion was maintained for 1 h with sporadic stirring. After extraction, a simple filtration was carried out and the filtrate was stored at -4 °C. Then, lyophilization was performed in order to obtain the dry extract. A Liotop machine (model L101) was used, reaching an average temperature of -52 °C.

The high molecular weight fraction (HMWF) was separated from the aqueous extract using an ultrafiltration process in which a specific porous membrane with a cut-off weight point of 3 kDa from Millipore-USA was employed. The HMWF was retained in the membrane using a centrifuge rotating at 3500 rpm for 40 min, stored at -4 °C and lyophilized.

Preparation of the specimens

The mild steel specimens have the following chemical composition (% m/m): C: 0.18, P: 0.04, S: 0.05, Mn: 0.30 and the remaining percentage of iron. For gravimetric tests, the specimens have rectangular shape of approximately 14 cm² in area. They were abraded with 100, 320 and 600 mesh size sandpapers, washed with distilled water and ethanol and dried in hot air. For the potentiodynamic polarization and electrochemical impedance spectroscopy (EIS) experiments, a mild steel working electrode of approximately 0.913 cm² of surface area was used. This electrode was also abraded with 100, 320 and 600 mesh size sandpapers, washed with distilled water and ethanol, and then dried in hot air.

Gravimetric essays

Essays at different concentrations were carried out in the absence and presence of 100, 200, 400 and 800 mg L⁻¹ of the dry extract, for 2, 6, 24 and 48 h of immersion at room temperature. Gravimetric tests with temperature variation were performed in the absence and presence of 200 mg L⁻¹ of the dry extract, at 35, 45, 55, 65 and 85 °C, for 2 h immersion time. A thermostat bath was used to control the temperature.^{26,31-35}

The weight-loss measurements were obtained according to ASTM G31-7,³⁶ using an analytical balance with accuracy of 0.1 mg. The area of the specimens was measured by using a digital pachymeter. After the immersion period, the specimens were washed with distilled water and ethanol, and dried in hot air. The inhibition efficiency (IE%) for all weight-loss essays was determined by equation 1.^{26,31-35}

$$IE(\%) = \frac{W_{\text{corr},0} - W_{\text{corr}}}{W_{\text{corr},0}} \times 100 \quad (1)$$

where, $W_{\text{corr}0}$ is the corrosion rate in the absence of inhibitor ($\text{g cm}^{-2} \text{h}^{-1}$) and W_{corr} is the corrosion rate in the presence of inhibitor.

The apparent activation energy (E_a) of the mild steel dissolution process in acid medium was calculated according to the Arrhenius equation (equation 2).^{26,31-35}

$$\log W_{\text{corr}} = \log A - \frac{E_a}{2.303RT} \quad (2)$$

where W_{corr} is the corrosion rate ($\text{g cm}^{-2} \text{h}^{-1}$), E_a is the apparent activation energy (kJ mol^{-1}), R is the ideal gas constant ($8.314 \text{ J K}^{-1} \text{ mol}^{-1}$), T is the absolute temperature (K) and A is the pre-exponential factor.

Each experiment was performed in triplicate. All results were expressed by the average and its respective standard deviation.

Electrochemical tests

Electrochemical tests were performed in a model Autolab PGSTAT 128N potentiostat/galvanostat with a Metrohm impedance module. Prior to each experiment, the open circuit potential (OCP) was stabilized for 8000 s. The electrochemical impedance measurements were performed in a frequency range from 100 kHz to 10 mHz, with 10 points *per* decade and amplitude of 10 mV (rms). Parameters such as double layer capacitance (C_{dl}) and charge transfer resistance (R_{ct}) were taken from Nyquist diagrams. The potentiodynamic polarization curves were obtained immediately after the impedance essays and were performed using a scan rate of 1 mV s^{-1} from -300 up to $+300$ mV in relation to the stable OCP. Parameters as corrosion current density (j_{corr}), corrosion potential (E_{corr}), anodic (β_a) and cathodic (β_c) Tafel constants were obtained by the Tafel extrapolation method. The electrochemical measurements were performed in a glass cell containing three electrodes: mild steel as the working electrode, saturated calomel electrode ($\text{Hg}/\text{Hg}_2\text{Cl}_2/\text{Cl}^-$) as reference and a platinum wire with large area as counter electrode. The electrochemical cell was placed in a Faraday cage. For the potentiodynamic polarization essays, IE% was calculated from the corrosion current densities obtained from the polarization curves by the Tafel extrapolation method, equation 3.^{26,31-35}

$$\text{IE} (\%) = \frac{j_{\text{corr}0} - j_{\text{corr}}}{j_{\text{corr}0}} \times 100 \quad (3)$$

where, $j_{\text{corr}0}$ is the corrosion current density (mA cm^{-2}) in the absence of the inhibitor and j_{corr} is the corrosion current

density in the presence of the inhibitor, obtained from the Tafel extrapolation.

The inhibition efficiency was calculated based on the values of the charge transfer resistance, according to equation 4.^{26,31-35}

$$\text{IE} (\%) = \frac{R_{ct} - R_{ct,0}}{R_{ct}} \times 100 \quad (4)$$

where $R_{ct,0}$ is the charge transfer resistance ($\Omega \text{ cm}^2$) obtained in the absence of the inhibitor and R_{ct} is the charge transfer resistance obtained in the presence of the inhibitor.

All electrochemical tests were also performed with the HMWF from the aqueous extract of cumaru seeds in order to investigate which compounds could be responsible by the inhibitory action of the extract.

Surface analysis by scanning electron microscopy (SEM)

The specimens used in the surface analysis were previously treated. They were abraded with 100, 320 and 600 mesh sandpapers and immersed in a 1 mol L^{-1} HCl solution in the absence and in the presence of 100 mg L^{-1} of the aqueous extract of cumaru seeds at room temperature for 2 h. After this period, the specimens were washed with double distilled water, acetone and dried in hot air. They were analyzed by scanning electron microscope Phenom ProX with an acceleration of 15 kV. An abraded specimen was analyzed without immersion in the HCl solution.

Chemical characterization of the aqueous extract of cumaru (*Dipteryx odorata*) seeds

IR spectra were obtained on a spectrometer with Fourier transform (FTIR) from Thermo Scientific model Nicolet 6700, with a wavenumber range from 400 to 4000 cm^{-1} , a resolution of 4 cm^{-1} and each spectrum was obtained from the average of 16 scans.

^1H , ^{13}C and 2D nuclear magnetic resonance (NMR) spectroscopic measurements were carried out at 298 K using a Bruker Avance III 500 MHz spectrometer. The sample was prepared by dissolving 20 mg of the dry aqueous cumaru seeds extract in 0.6 mL D_2O . The spectra were referenced to tetramethylsilane. Chemical shifts (δ) are given in parts *per* million (ppm).

Results and Discussion

The aqueous extract of cumaru seeds was tested to inhibit corrosion of mild steel in 1 mol L^{-1} HCl acid solution. The inhibitory effect was investigated using weight-loss

essays, open circuit potential (OCP), polarization curves and electrochemical impedance measurements.

Gravimetric essays results

Effect of inhibitor concentration and immersion time

Results of weight-loss essays for mild steel immersed in 1 mol L⁻¹ HCl solution in the absence and presence of the dry extract of cumaru and its HMWF can be seen in Table 1. The experiments were carried out at 25 °C, with different immersion times (2, 6, 24 and 48 h) and inhibitor concentrations (100, 200, 400 and 800 mg L⁻¹).

In all tests, it is observed that the corrosion rate of the mild steel in acid medium decreases with the addition of the dry extract of cumaru, showing that the compounds present in the aqueous extract of cumaru seeds inhibit the corrosion of the mild steel in acid solution. Inhibition efficiency increased with immersion time, stabilizing a maximum value in 24 h. These results show that the adsorption of the molecules on the surface of mild steel takes some time to reach saturation.³⁷ The immersion time significantly influences the IE, whereas the increase of the dry extract concentration has a lower effect on the IE. The HMWF, in particular, reaches 98% of IE after 6-h immersion time. Even at low concentration (100 mg L⁻¹), both aqueous extract of cumaru seeds and its HMWF formed an inhibitory film that adsorbs on the metal surface, leading to an IE of 96% in 24 h of immersion in the presence of the dry extract and 98% in only 6 h of immersion in the presence of its HMWF. For the aqueous extract of cumaru seeds, the maximum efficiency (98%) is achieved using 800 mg L⁻¹, after longer immersion time, 24 h. The percentual keeps constant with 48 h immersion time. This behavior has also been reported by Singh and Ebenso.³⁸

The high molecular weight fraction always presented inhibition efficiency values higher than the aqueous extract of cumaru seeds, in all concentrations and immersion times, as can be seen in Table 1. These results suggest that macromolecules may be adsorbed in the metal surface, inhibiting the corrosive process. Maximum efficiency (99%) is achieved using more concentrated solutions (400-800 mg L⁻¹) for longer immersion times.

Effect of temperature

The effect of temperature on mild steel corrosion in 1 mol L⁻¹ HCl solution was evaluated from 35 to 85 °C, with 2 h of immersion. The results are shown in Table 2. The corrosion rate of mild steel increases with temperature, in both absence and presence of the dry extract of cumaru seeds and its HMWF, being more significant in the presence of the extract. Yaro *et al.*³⁹ observed similar results in

Table 1. Results of weight-loss measurements of mild steel immersed in 1 mol L⁻¹ HCl solution, in the absence and presence of the dry extract of cumaru and its HMWF, at different concentrations and immersion times

time / h	[Inhibitor] / (mg L ⁻¹)	W _{corr} / (g cm ⁻² h ⁻¹)	IE / %	SD _{IE}
	0	1.34 × 10 ⁻³	–	–
	Aqueous cumaru seeds extract			
	100	2.78 × 10 ⁻⁴	79.2	1.7
	200	2.64 × 10 ⁻⁴	80.3	1.4
	400	1.68 × 10 ⁻⁴	87.5	1.3
2	800	1.57 × 10 ⁻⁴	88.3	4.5
	HMWF			
	100	1.61 × 10 ⁻⁴	88.0	0.5
	200	1.50 × 10 ⁻⁴	88.8	0.0
	400	9.25 × 10 ⁻⁵	93.1	0.8
	800	8.55 × 10 ⁻⁵	93.6	2.6
	0	2.78 × 10 ⁻³	–	–
	Aqueous cumaru seeds extract			
	100	3.05 × 10 ⁻⁴	89.0	2.2
	200	2.31 × 10 ⁻⁴	91.7	3.1
	400	2.34 × 10 ⁻⁴	91.6	1.9
6	800	2.22 × 10 ⁻⁴	92.0	1.3
	HMWF			
	100	6.70 × 10 ⁻⁵	97.6	0.3
	200	6.80 × 10 ⁻⁵	97.9	0.1
	400	6.00 × 10 ⁻⁵	97.8	0.3
	800	5.65 × 10 ⁻⁵	97.7	0.2
	0	1.21 × 10 ⁻³	–	–
	Aqueous cumaru seeds extract			
	100	4.68 × 10 ⁻⁵	96.1	0.1
	200	4.02 × 10 ⁻⁵	96.7	0.4
	400	3.55 × 10 ⁻⁵	97.1	0.2
24	800	2.87 × 10 ⁻⁵	97.6	0.2
	HMWF			
	100	1.95 × 10 ⁻⁵	98.4	0.2
	200	1.60 × 10 ⁻⁵	98.7	0.3
	400	7.00 × 10 ⁻⁶	99.4	0.7
	800	9.00 × 10 ⁻⁶	99.3	0.2
	0	1.26 × 10 ⁻³	–	–
	Aqueous cumaru seeds extract			
48	100	4.87 × 10 ⁻⁵	96.1	0.1
	200	4.20 × 10 ⁻⁵	96.6	0.1
	400	3.60 × 10 ⁻⁵	97.2	0.0
	800	2.70 × 10 ⁻⁵	97.6	0.1

W_{corr}: corrosion rate; IE: inhibition efficiency; SD_{IE}: standard deviation; HMWF: high molecular weight fraction.

their study. These results explain the decrease of IE with temperature, suggesting that the molecules are desorbing from the metal surface as the temperature increases. It is directly related to the physical adsorption mechanism whose interaction between the inhibitory molecules and the metal surface is electrostatic, which leads to desorption of the molecules at high temperatures due to the increased molecular agitation.^{40,41} It was observed that this behavior is less pronounced in the presence of the high molecular weight fraction, with little variation in the IE as the temperature increases. This suggests that macromolecules such as carbohydrates may be doing a more intense physical interaction with the metal surface, inhibiting the corrosive process.

Table 2. Corrosion rates of mild steel in 1 mol L⁻¹ HCl solution, in the absence and presence of the dry extract of cumaru seeds and its HMWF, at different temperatures

Temperature / °C	Blank $W_{\text{corr}} /$ (g cm ⁻² h ⁻¹)	$W_{\text{corr}} /$ (g cm ⁻² h ⁻¹)	IE / %	SD _{IE}
Aqueous cumaru seeds extract				
35	2.91×10^{-3}	3.30×10^{-4}	88.7	1.1
45	5.81×10^{-3}	5.53×10^{-4}	90.5	1.7
55	9.73×10^{-3}	1.13×10^{-3}	88.4	1.2
65	1.52×10^{-2}	2.79×10^{-3}	81.6	1.9
85	3.30×10^{-2}	1.07×10^{-2}	67.6	0.1
HMWF				
35	3.31×10^{-3}	1.80×10^{-4}	94.6	0.4
45	6.23×10^{-3}	2.98×10^{-4}	95.2	0.3
55	9.99×10^{-3}	7.56×10^{-4}	92.4	0.7
65	1.48×10^{-2}	1.14×10^{-3}	92.3	0.1
85	3.11×10^{-2}	3.57×10^{-3}	88.5	0.4

W_{corr} : corrosion rate; IE: inhibition efficiency; SD_{IE}: standard deviation; HMWF: high molecular weight fraction.

Arrhenius plots are presented in Figure 1 showing ($\ln W_{\text{corr}}$) versus ($1/T$) for mild steel immersed in a 1 mol L⁻¹ HCl solution in the absence and presence of 200 mg L⁻¹ of the dry extract of cumaru and its HMWF. The apparent activation energy obtained in the blank essay was 42.2 kJ mol⁻¹ (Table 3). The addition of the dry extract and its HMWF increased to 65.5 and 55.6 kJ mol⁻¹, respectively. The higher values of the apparent activation energy in the presence of the inhibitors can be interpreted as the occurrence of physical adsorption, as previously mentioned.^{23,42}

A criterion for the purely blocking mechanism is that the inhibitor does not affect the effective activation energy of the corrosion process. It should be noted that blocking inhibitors rarely occur.²⁶⁻⁴³ Most of the organic compounds

are mixed-type inhibitors. In this case, the screening effect is added to the activation effect. Both dry extract and its HMWF act by a mixed-type mechanism since the apparent activation energy increased with their addition.

The activation parameters ΔH^* and ΔS^* were obtained from an alternative relation of the Arrhenius equation, showed in equation 5:

$$W_{\text{corr}} = RT/Nh \exp(\Delta S^*/R) \exp(-\Delta H^*/RT) \quad (5)$$

where h is the Planck constant (6.63×10^{-34} J s), N is the Avogadro number (6.02×10^{23}), ΔS^* is the activation entropy and ΔH^* is the activation enthalpy.

Table 3 shows the thermodynamic activation parameters obtained through the alternative Arrhenius equation (equation 5). A higher value of E_a and ΔH^* was observed in the presence of both inhibitors, showing again a physical interaction between the mild steel and the molecules present in the cumaru extract. The values of E_a are greater than the corresponding values of ΔH^* , showing that the corrosion process must involve a gas reaction, the evolution of hydrogen gas, associated with a decrease in the total reaction volume.^{32,35,44} Furthermore, the difference between E_a and ΔH^* is 2.8 kJ mol⁻¹, which is practically equal to the average value of RT (2.74 kJ mol⁻¹) indicating that the corrosion process is a unimolecular reaction.^{26-28,31-35}

Electrochemical results

Open circuit potential (OCP)

Prior to EIS measurements, OCP plots of mild steel in 1 mol L⁻¹ HCl solution (Figure 2) were recorded in the absence and presence of the dry extract of cumaru seeds and its HMWF. For the blank essay, the open circuit potential stabilized around 5000 s. In the absence of inhibitor, it is observed a variation of potential in the first hour of immersion towards negative values, which indicates air-formed oxide dissolution in HCl solution, and then stabilization in approximately -525 mV. This variation of potential towards negative values in the first seconds is no longer observed with the addition of the inhibitors. In general, for the dry extract of cumaru seeds there is an increase of OCP in the first few seconds with stabilization at -522, -496, -498 and -535 mV using 100, 200, 400 and 800 mg L⁻¹ of the inhibitor, respectively, and a maximum displacement of +34 mV at 200 mg L⁻¹. In the presence of the HMWF, the OCP stabilized between -522 and -543 mV for 100 and 800 mg L⁻¹ with a maximum displacement of -13 mV at 800 mg L⁻¹. These results show a slight anodic and cathodic shift with respect to the blank for cumaru extract and its HMWF, respectively, demonstrating that

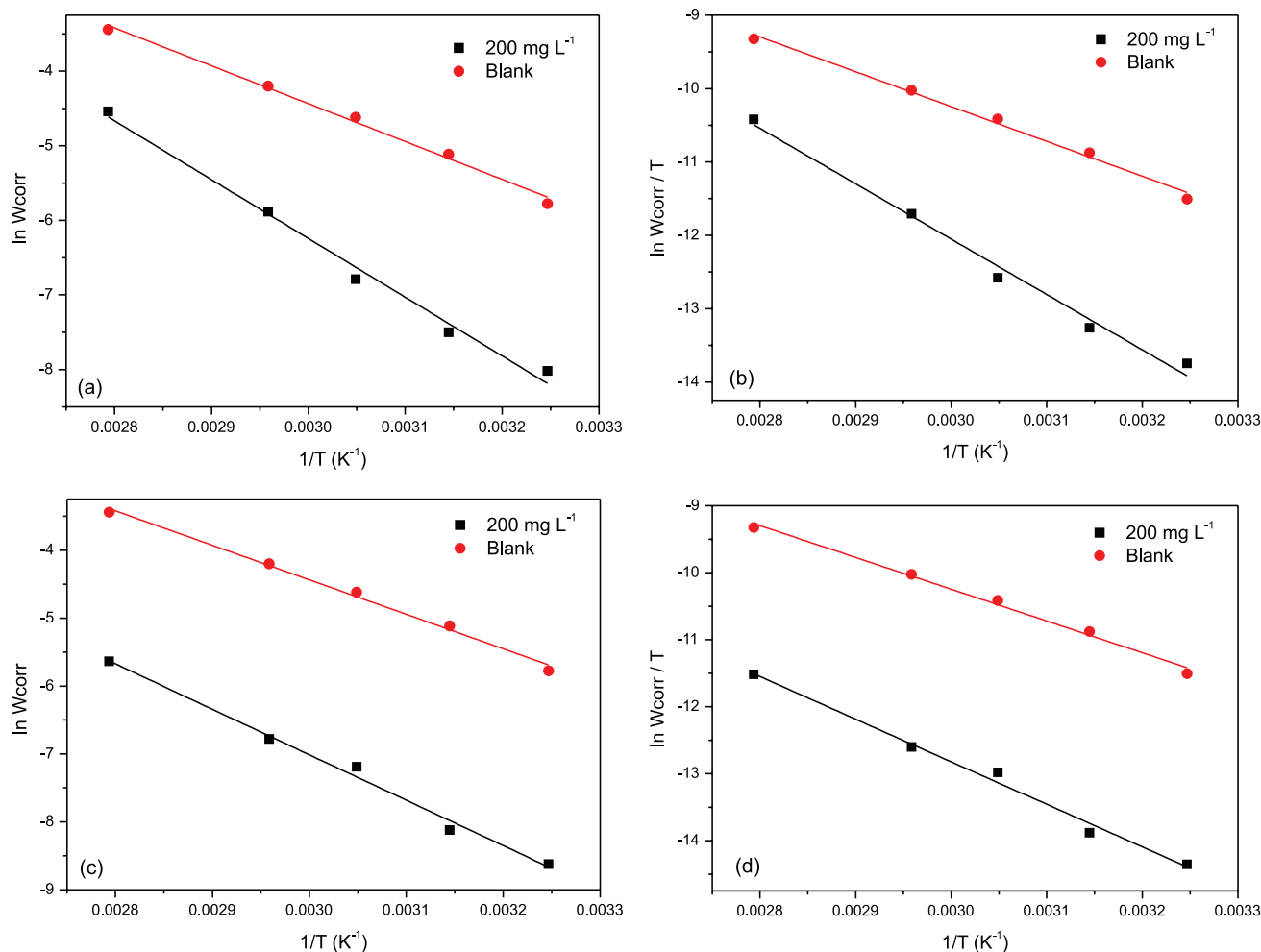


Figure 1. Arrhenius plots: (a) $\ln W_{\text{corr}} \times 1/T$ and (b) $\ln (W_{\text{corr}}/T) \times 1/T$ for mild steel in 1 mol L⁻¹ HCl solution in the absence and presence of the dry extract of cumaru seeds; and (c) $\ln W_{\text{corr}} \times 1/T$ and (d) $\ln (W_{\text{corr}}/T) \times 1/T$ for mild steel in 1 mol L⁻¹ HCl solution in the absence and presence of the HMWF of the aqueous extract of cumaru seeds.

Table 3. Values of E_a and thermodynamic activation functions (ΔH^* and ΔS^*) for the corrosion process of mild steel in 1 mol L⁻¹ HCl solution in the absence and presence of the inhibitors

	E_a / (kJ mol ⁻¹)	ΔH^* / (kJ mol ⁻¹)	ΔS^* / (J K ⁻¹ mol ⁻¹)
Blank essay	42.2	39.5	-164.4
With dry extract of cumaru seeds	65.5	62.8	-109.5
With HMWF of aqueous extract of cumaru	55.6	52.9	-145.6

E_a : activation energy; ΔH^* : activation enthalpy; ΔS^* : activation entropy; HMWF: high molecular weight fraction.

the extract acts by the adsorption of organic compounds present in both inhibitors.

Electrochemical impedance spectroscopy (EIS)

Figure 3 shows the Nyquist diagrams, obtained from the immersion of mild steel in 1 mol L⁻¹ HCl solution in the absence and presence of the dry extract of cumaru seeds and its HMWF.

Analyzing the Nyquist diagrams, it is observed that the diagrams are similar, both in the absence and presence of

the inhibitors, indicating the activation-controlled nature of the reaction during a one-charge transfer process even in the presence of the inhibitors.^{32,35,42,45} Figures 3a and 3b show only one capacitive loop, which can be related to a single time constant attributed to the charge transfer and the double layer capacitance, being the corrosive process of the mild steel in acid medium under charge transfer control.⁴⁶ This capacitive loop is flattened both in the absence and presence of the inhibitors. Such behavior is characteristic of solid electrodes due to the surface roughness of the steel

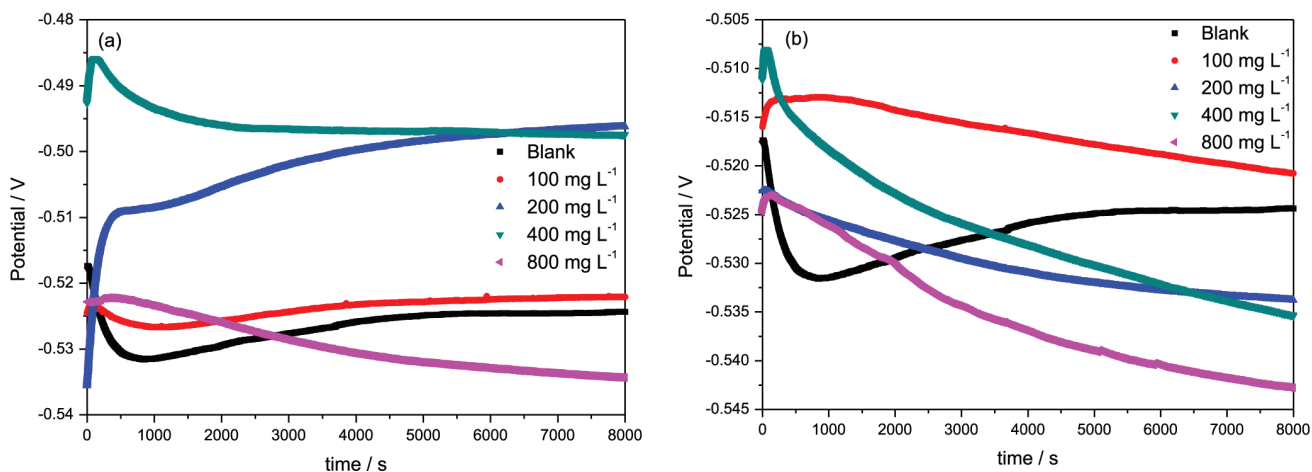


Figure 2. OCP plots of mild steel samples in 1 mol L^{-1} HCl solution in the absence and presence of different concentrations of the dry extract of cumaru seeds (a) and its HMWF (b).

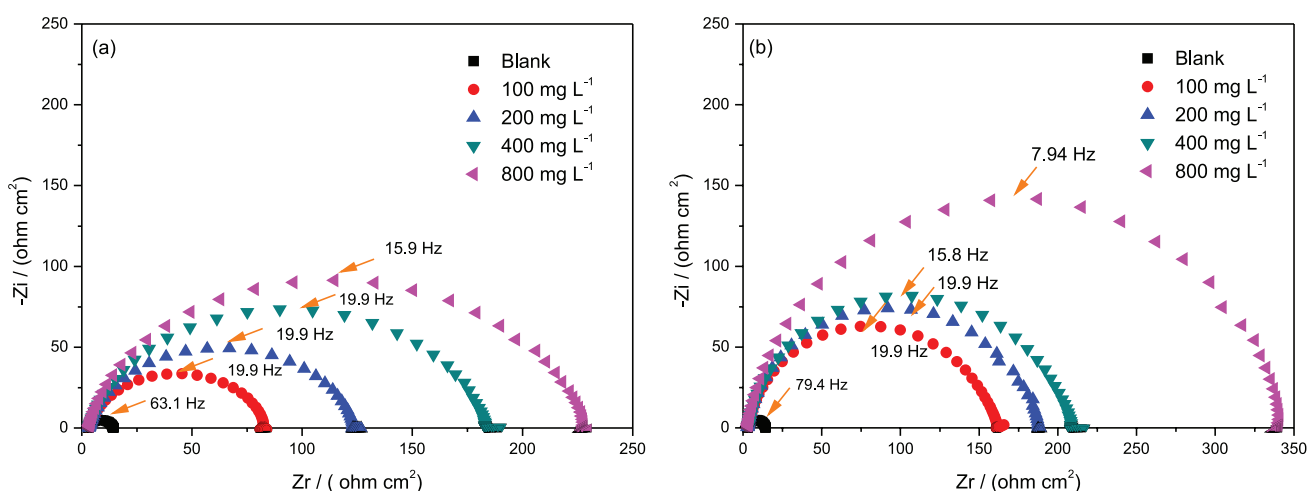


Figure 3. Nyquist diagrams for mild steel immersed in 1 mol L^{-1} HCl solution in the absence and presence of the inhibitors at different concentrations: (a) dry extract of cumaru seeds and (b) HMWF of the aqueous extract of cumaru. The total immersion time at which the spectra were recorded was 8000 s.

during corrosive process.¹⁷ The presence of the inhibitors increases significantly the loop diameter compared to the blank test, showing that the corrosive process is inhibited by the molecules present in the dry extract and in its HMWF.

The Nyquist diagrams of the inhibitors also indicate an increase in the values of charge transfer resistance as the concentration of the inhibitors enhances. Comparing the R_{ct} obtained using 400 and 800 mg L^{-1} of both inhibitors, it can be seen a more pronounced increase in the experiment carried out with the HMWF of the aqueous extract of cumaru seeds. Table 4 shows the electrochemical impedance results. In the experiments with 800 mg L^{-1} of inhibitor, the R_{ct} was 277 and $417 \Omega \text{ cm}^2$, for the dry extract of cumaru seeds and its HMWF, respectively. This behavior in the R_{ct} value using the HMWF can be attributed to the presence of molecules with higher molecular weight. As far as we know, there are no studies in the literature reporting the chemical composition of aqueous extract of cumaru

(*Dipteryx odorata*) seeds. In this work, a preliminary characterization of the dry extract was done by FTIR, ^1H , ^{13}C and 2D NMR. The results will be discussed later, but it can be said that the data suggest the predominance of carbohydrates. Based on this, it can be suggested that the rise in the R_{ct} value in the presence of 800 mg L^{-1} of HMWF would be associated with a higher concentration of this class of compounds in the fraction. The highest inhibition efficiency obtained with the HMWF was also observed in previous studies by our group.^{26,32-35}

The presence of the inhibitors in the 1 mol L^{-1} HCl solution causes an increase in the impedance modules in the lower frequency range, showing their inhibitory action on the corrosive process of mild steel in the acid medium, probably by the adsorption of the constituents of the extract (Bode diagrams can be seen on Supplementary Information section). All diagrams presented a single time constant around 100 Hz region which could be

associated to the charge transfer process with a small shift for lower frequency in the presence of both inhibitors. It is represented by an one-wave curve, that increases in height as the concentration of the inhibitor increases, enhancing the capacitive behavior of the interface, which indicates more molecules adsorbed on mild steel surface at higher inhibitors concentrations.^{44,47,48} The value of the phase angle obtained for the free-inhibitor essay was approximately 40°. The addition of both inhibitors in the solution increased the phase angle value, peaking up to 70° using 800 mg L⁻¹ of the inhibitor. These results confirm the inhibitory action of the molecules upon the metal surface, which reduces the active sites susceptible to corrosion attack.

All electrochemical impedance diagrams were based on an equivalent circuit shown in Figure 4, where R_s is the ohmic solution resistance, R_{ct} is the charge transfer resistance and CPE is the constant phase element. The double layer capacitance (C_{dl}) was calculated following equation 6.^{26,31-35}

$$C_{dl} = Y_0(2\pi f_{max})^{n-1} \quad (6)$$

where Y_0 is the magnitude of the CPE, n represents the deviation from ideality, and f_{max} is the frequency in which the imaginary impedance component is maximum.

Table 4 shows that increasing inhibitor concentration, the frequency (f_{max}) and the double layer capacitance (C_{dl}) decrease and the charge transfer resistance increases, leading to an inhibition efficiency (IE) increase. These results indicate that molecules present in the inhibitors adsorb on the mild steel surface, blocking the surface of

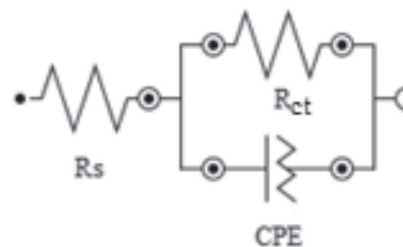


Figure 4. Equivalent circuit used to interpret electrochemical impedance results.

the steel and hindering the charge transfer. It is noted that the inhibition efficiency values for all concentrations of inhibitors were high. These results show that probably the macromolecules are responsible for the inhibitory action of the aqueous extract of cumaru seeds. The best IE results were 94.7 and 96.5% at a concentration of 800 mg L⁻¹ of the dry extract of cumaru seeds and its HMWF, respectively.

These inhibitors are mixed-type where the screening effect is added to the activation effect. Both the dry extract and its HMWF act by a mixed-type mechanism since the apparent activation energy increased with their addition. The C_{dl} and R_{ct} results corroborate this statement. If the inhibitors showed the pure blocking effect, acting only by surface screening, both C_{dl} and R_{ct} would have their values constant and equal to the blank results with the correction of the electroactive area, i.e., normalizing these two quantities by $(1 - \theta)$, being θ (fraction of the surface covered) determined by weight-loss measurements (data for 2 h in Table 1).⁴⁴ Table 5 shows that mainly the C_{dl} values do not keep constant with the area normalization.

Table 4. Electrochemical impedance results for mild steel immersed in 1 mol L⁻¹ HCl solution in the absence and presence of the dry extract of cumaru seeds and its HMWF

[Inhibitor] / (mg L ⁻¹)	f_{max} / Hz	C_{dl} / ($\mu\text{F cm}^{-2}$)	Y_0 / ($\mu\text{mho s}^n \text{cm}^{-2}$)	n	R_{ct} / (Ωcm^2)	IE / %	SD _{IE}
0	73.4	179	292	0.904	14.8	–	–
Aqueous cumaru seeds extract							
100	19.9	68.2	139	0.875	98.6	84.9	2.4
200	19.9	62.3	105	0.873	132	88.8	4.1
400	19.9	46.9	81.1	0.868	199	92.6	0.6
800	15.9	45.2	62.0	0.885	277	94.7	0.2
HMWF							
100	19.9	57.1	84.1	0.876	195	91.0	0.9
200	19.9	44.9	64.0	0.883	227	93.5	0.5
400	15.8	47.9	67.4	0.880	253	94.2	0.6
800	7.94	49.0	64.9	0.894	417	96.5	0.4

f_{max} : maximum frequency; C_{dl} : double layer capacitance; Y_0 : magnitude of the CPE; n : deviation from ideality; R_{ct} : charge transfer resistance; IE: inhibition efficiency; SD_{IE}: standard deviation; HMWF: high molecular weight fraction.

Table 5. Normalized R_{ct} and C_{dl} obtained for mild steel immersed in 1 mol L⁻¹ HCl solution in the absence and presence of the dry extract of cumaru and its HMWF considering the fraction of the surface covered by adsorbed molecules (θ) from the weight-loss measurements with 2 h immersion time

[Inhibitor] / (mg L ⁻¹)	θ	(1- θ)	Normalized R_{ct} / (Ω cm ²)	Normalized C_{dl} / (μ F cm ⁻²)
0	–	–	14.8	179
Aqueous cumaru seeds extract				
100	0.792	0.208	20.5	328
200	0.803	0.197	26.0	316
400	0.875	0.125	24.9	375
800	0.883	0.117	32.4	386
HMWF				
100	0.880	0.120	23.4	476
200	0.888	0.112	25.4	401
400	0.931	0.069	17.5	694
800	0.936	0.064	26.7	766

θ : fraction of the surface covered; R_{ct} : charge transfer resistance; C_{dl} : double layer capacitance; HMWF: high molecular weight fraction.

Adsorption isotherm

Adsorption is a phenomenon observed when a substance concentrates at the interface between two phases. This adsorption can be physical or chemical; it will depend on the type of the force responsible for the phenomenon. Physical adsorption is a reversible process whereas chemical adsorption can lead to an irreversible reaction. Gravimetric tests with temperature variation showed that the adsorption of the constituents of the aqueous extract of cumaru seeds on the metal surface is physical. The interaction between the inhibitors and the mild steel surface was examined by the adsorption isotherms during the corrosion process. The experimental results were adjusted to different adsorption isotherms (Langmuir, El-Awady, Flory-Huggins, Temkin and Frunkim), in order to study the adsorption behavior of the constituents of the aqueous extract of cumaru seeds. The inhibition efficiency is directly proportional to the fraction of the surface covered by adsorbed molecules (θ), which was calculated according to equation 7, using the R_{ct} values from the impedance diagrams, shown in Table 4.

$$\theta = \frac{IE (\%)}{100} \quad (7)$$

These adsorption isotherms are commonly used. They relate the degree of coverage of the mild steel surface by the inhibitor molecules to the inhibitor concentration. The equations 8-12 show this relation:

$$\text{Langmuir isotherm: } \frac{C}{\theta} = \frac{1}{K_{ads}} + C \quad (8)$$

$$\text{El-Alwady isotherm: } \log\left(\frac{\theta}{1-\theta}\right) = \log K_{ads} + y \log C \quad (9)$$

$$\text{Flory-Huggins isotherm: } \log\left(\frac{\theta}{C}\right) = \log K_{ads} + x \log(1-\theta) \quad (10)$$

$$\text{Temkin isotherm: } \theta = \left(\frac{-2.303}{2a}\right) \log K_{ads} + \left(\frac{-2.303}{2a}\right) \log C \quad (11)$$

$$\text{Frunkim isotherm: } \log\left[\left(\frac{\theta}{1-\theta}\right)C\right] = \log K_{ads} + g\theta \quad (12)$$

where C is the inhibitor concentration, K_{ads} is the adsorption constant, a and g are the lateral parameter of interaction between the adsorbed molecules, x is the number of adsorbed water molecules substituted by inhibitor molecules, and y is the number of adsorbed molecules in each active site.^{26,35}

The value of the linear correlation coefficient (R) determines the isotherm that best fit the experimental data. Table 6 shows the straight-line equations and the values of the coefficient of correlation for the experiments with the dry extract of cumaru seeds and its HMWF as inhibitors.

Langmuir isotherm assumes a homogeneous surface where the adsorption sites are energetically identical. The adsorption occurs in monolayers and the adsorbed molecules do not interact with each other.^{17,20,49} The isotherms of Flory-Huggins and El-Awady^{50,51} consider that an active site can be occupied by more than one inhibitor molecule or that a single inhibitor molecule can adsorb in more than one active site (x and y parameters, respectively). For the isotherm of Flory-Huggins, x values greater than one unit indicate that more than one water molecule has been replaced by an inhibitor one, while for the isotherm

Table 6. Data of the isotherms obtained by linear adjustments in the experiments with the dry extract of cumaru seeds and with its HMWF as inhibitors

Isotherm	Dry extract		HMWF	
	Line equation	R	Line equation	R
Langmuir	$y = 1.033x + 14.29$	0.999	$y = 1.029x + 8.125$	0.999
El-Awady	$y = 0.557x - 0.317$	0.998	$y = 1.029x + 8.125$	0.817
Flory-Huggins	$y = 1.861x - 0.464$	0.998	$y = 0.359x - 0.336$	0.807
Temkin	$y = 0.099x + 0.669$	0.991	$y = 2.521x + 0.656$	0.895
Frumkin	$y = -0.071x + 0.069$	0.992	$y = 0.042x + 0.837$	0.632

HMWF: high molecular weight fraction; R: linear correlation coefficient.

of El-Awady, y values less than one unit show that a single molecule involved in the adsorption process has been adsorbed in more than one active site. According to the line equations of Flory-Huggins and El-Awady isotherms, x value was 1.861 and y value was 0.557, respectively. These results suggest that the adsorbed molecules present in the dry extract are bulky and occupy more than one active site. Temkin's isotherm assumes that the heat of adsorption of all molecules covering the adsorbent decreases linearly as a function of coating, due to interactions between the adsorbed molecules ($a > 0$, attraction; $a < 0$, repulsion).⁵² Considering the result obtained in the presence of the inhibitor, where a value was negative, a repulsive interaction between the adsorbed molecules could be considered. Frumkin's isotherm is an optimized model of Langmuir, reducing some parameters. This isotherm correlates the adsorbed surface density with the concentration of the investigated chemical species in the solution. The slope of the line (g) gives the degree of lateral interaction.⁵³ The negative sign indicates that the interaction between the adsorbed molecules on the metal surface is repulsive.⁵⁴

According to Souza *et al.*,⁵⁵ acceptable correlation coefficients generally fall between 0.99 and 0.60. For this study, all isotherms showed a reasonable fitting line in the presence of the dry extract of cumaru seeds (Table 6). The best fitting line to the experimental values was Langmuir isotherm, showing good linearity ($R = 0.999$) and an angular coefficient value of 1.033. This result suggests the formation of a protective monolayer on the metal surface, probably involving bulky molecules. The adsorption constant (K_{ads}) obtained from the Langmuir isotherm adjustment was 0.069 L mg^{-1} for experiments with the dry extract of cumaru seeds as inhibitor. K_{ads} is the equilibrium constant of the adsorption process and it is related to the adsorption free energy (ΔG_{ads}°). As the molecular weight of the adsorbed species on the metal surface as well as its content in the extract are not known, the calculation of ΔG_{ads}° cannot be done.^{17-20,26,35,45} Once the study with temperature variation proved that the adsorption has a physical nature, the formation of multilayers is also plausible.

The isotherm that best adjusted the experimental data using the HMWF as inhibitor was also the Langmuir isotherm. The coefficient of correlation (R) was 0.999 (Table 6). The adsorption constant (K_{ads}) obtained from the Langmuir isotherm adjustment was 0.123 L mg^{-1} for the set of experiments with the HMWF. The angular coefficient was slightly greater than one; in this case, the existence of interactions between the adsorbed molecules and/or the possibility of more than one of inhibitory molecules occupying an active site can be considered.^{26,56}

Potentiodynamic polarization measurements

Figure 5 exhibits the polarization curves of mild steel in 1 mol L^{-1} HCl solution, in the absence and presence of different inhibitor concentrations (100, 200, 400 and 800 mg L^{-1}). Kinetic parameters, such as corrosion potential (E_{corr}), current density (j_{corr}), Tafel anodic (β_a) and cathodic (β_c) constants, were obtained using the Tafel extrapolation method. Using the j_{corr} values, it was possible to calculate the inhibition efficiency (IE) of the corrosive process. All these parameters are presented in Table 7.

Analyzing the Figure 5, it is possible to observe that by adding the inhibitors to the acid solution, there was a displacement of the anodic and cathodic polarization curves to lower current densities showing that both reactions are inhibited by both the dry extract of cumaru seeds and its HMWF. In Figures 5a and 5b, it is observed that the cathodic branch is most affected by the presence of the inhibitor, characterizing the dry extract of cumaru seeds and its HMWF as a mixed-type inhibitor with prominent action in the cathodic branch.^{35,57-60}

In general, the increase of the inhibitor concentration in the corrosive medium causes a decrease of the corrosion current density, which reflects in the increase of IE. It can be explained by the formation of a protective adsorbed film, consisting of molecules from the aqueous extract of cumaru seeds, on the metal surface that is responsible for the retardation of the corrosion process. Table 7 shows a slight change in the Tafel slopes (β_a and β_c) with the inhibitors

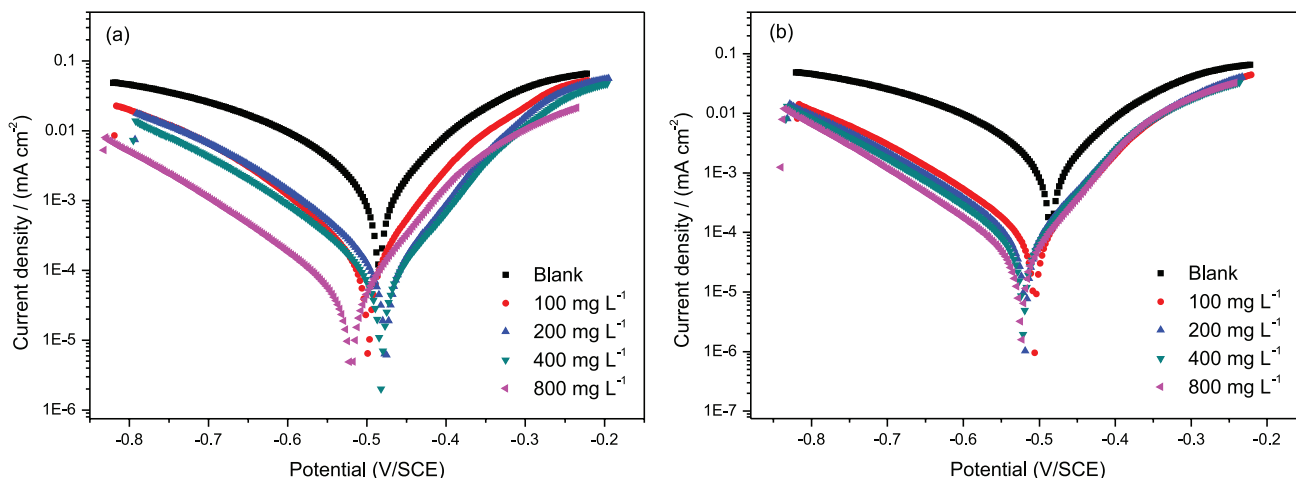


Figure 5. Polarization curves of mild steel in 1 mol L⁻¹ HCl solution in the absence and presence of different concentrations of (a) dry extract of cumaru seeds and (b) its HMWF. The total immersion time at which the spectra were recorded was 9500 s.

Table 7. Kinetic parameters obtained from the Tafel plots for mild steel in 1 mol L⁻¹ HCl solution in the absence and presence of the dry extract of cumaru and its HMWF at different concentrations

[Inhibitor] / (mg L ⁻¹)	E _{ocp} / mV	E _{corr} / mV	j _{corr} / (mA cm ⁻²)	β _a / (mV dec ⁻¹)	-β _c / (mV dec ⁻¹)	IE / %	SD _{IE}
0	-525	-491	8.75 × 10 ⁻⁴	80.7	105	-	-
Aqueous cumaru seeds extract							
100	-522	-498	1.91 × 10 ⁻⁴	67.7	143	78.2	0.3
200	-496	-477	1.51 × 10 ⁻⁴	68.8	151	82.7	2.7
400	-498	-482	9.77 × 10 ⁻⁵	71.8	146	88.8	0.2
800	-535	-520	6.38 × 10 ⁻⁵	69.3	135	92.7	0.2
HMWF							
100	-522	-506	1.03 × 10 ⁻⁴	84.2	137	88.2	0.4
200	-534	-518	8.65 × 10 ⁻⁵	80.8	137	90.1	0.2
400	-537	-521	6.75 × 10 ⁻⁵	83.0	130	92.3	0.4
800	-543	-524	5.52 × 10 ⁻⁵	86.4	126	93.7	0.4

E_{ocp}: open circuit potential; E_{corr}: corrosion potential; j_{corr}: current density; β_a: Tafel anodic constant; β_c: Tafel cathodic constant; IE: inhibition efficiency; SD_{IE}: standard deviation; HMWF: high molecular weight fraction.

addition, suggesting that the inhibitors molecules adsorption on the metal surface could occur without modification of the corrosion process mechanism, although the E_a obtained in the presence of both inhibitors was higher than in their absence.

The increment in the concentration of the dry extract resulted in a decrease of the current density when compared to blank, increasing the inhibition efficiency. The maximum IE value was 92.7% at 800 mg L⁻¹ of the inhibitor, which confirms the previous discussion concerning the formation of the protective film. The HMWF showed the same behavior of the dry extract, corroborating the results of weight-loss measurements and EIS. It is noted that the IE values for all concentrations of the HMWF were high, reaching 93.7% at a concentration of 800 mg L⁻¹. Comparing the results shown in Table 7, it is observed that at low concentrations, as 100 mg L⁻¹ for example, an IE of 88.2% was obtained for the HMWF test, confirming

the previous discussion in which molecules with high molecular weight would be responsible for this inhibition and protection of mild steel.

Surface analysis by SEM

Figure 6 shows micrographs of the abraded mild steel surface (Figure 6a), after its immersion in the HCl solution (blank) (Figure 6b), in the presence of 100 mg L⁻¹ of the dry cumaru extract (Figure 6c) and of HMWF (Figure 6d).

Figure 6b shows that the mild steel surface suffered severe corrosion at some points of the specimen when immersed in the hydrochloric acid solution. It is possible to observe a high roughness related to the attack of the HCl solution on the surface of mild steel, which previously had some grooves due to the abrading process, Figure 6a. In the presence of 100 mg L⁻¹ of the dry extract of cumaru

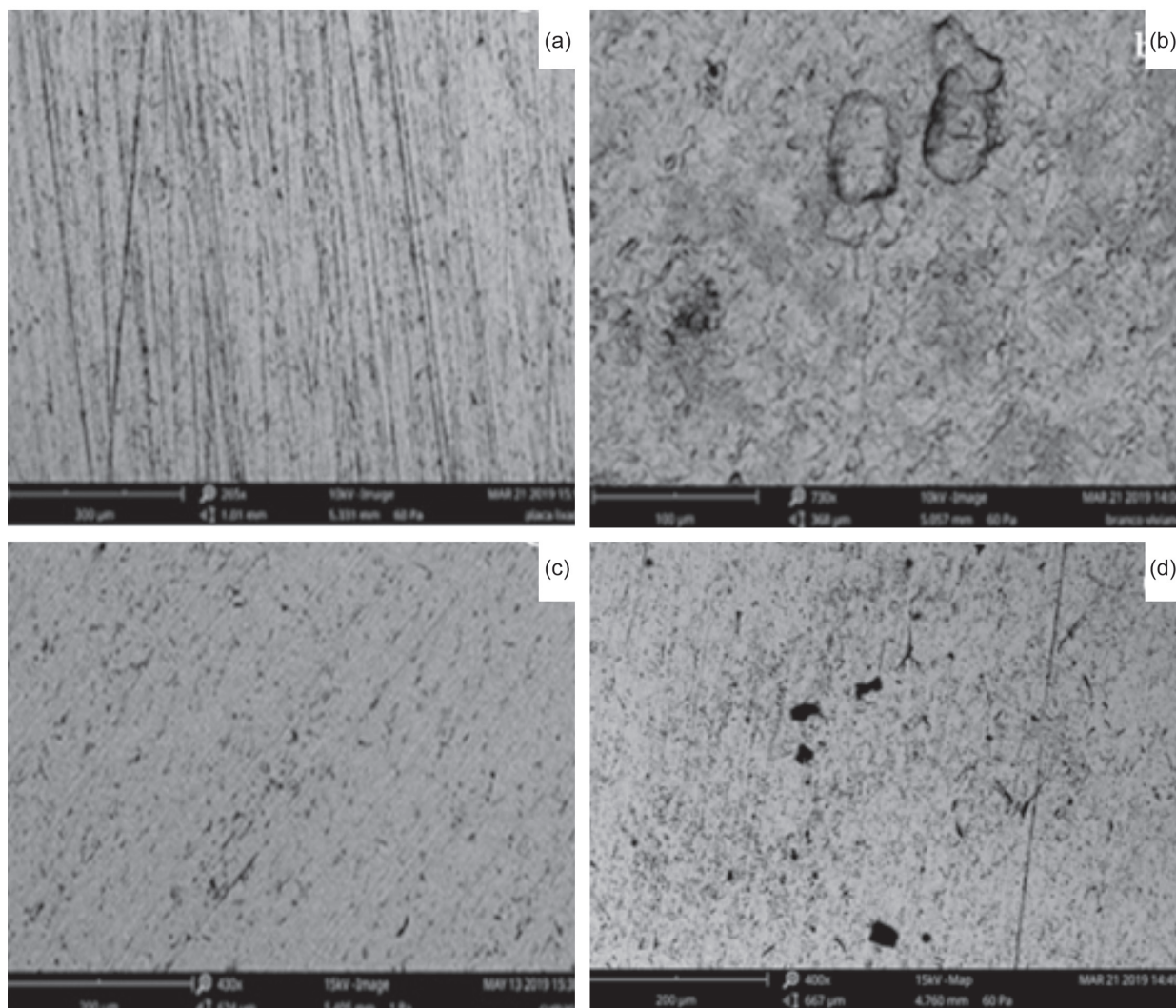


Figure 6. Surface micrographs of the mild steel where (a) the surface was just abraded; (b) the surface after immersion in the HCl 1 mol L⁻¹ solution; (c) the surface after immersion in the acid solution containing 100 mg L⁻¹ of the dry extract of cumaru seeds; and (d) the surface after immersion in the acid solution containing 100 mg L⁻¹ of the HMWF of the extract. The immersion was maintained for 2 h at room temperature.

seeds, the surface is much less rough and more uniform (Figure 6c), still being able to observe the abrading lines as those observed in Figure 6a. It should be associated with a lower rate of the corrosion process, where possibly molecules present in the extract of cumaru formed a protective layer on the mild steel surface, blocking the charge transfer. In the presence of 100 mg L⁻¹ of the HMWF of the cumaru extract (Figure 6d), it is possible to observe a surface covered by a thicker film than that found in Figure 6c where the abrading lines are smoothed. This thick film may be responsible for the higher IE observed with HMWF addition. It is still evident in the image the presence of black spots, possibly small holes present in the steel, that in the sanding process it was not possible to remove and not even noticed in time.

The analysis of the surface corroborates the weight-loss measurements and the electrochemical results, which

showed that the aqueous extract of cumaru seeds and its HMWF are effective in protecting the surface of mild steel in 1 mol L⁻¹ HCl solution, acting as good inhibitors and the superior inhibitory action of the HMWF.

Chemical characterization of aqueous extract of cumaru (*Dipteryx odorata*) seeds

Some phytochemical studies of *Dipteryx odorata* have been reported in the literature and several classes of compounds have been identified in different parts of the species. Griffiths⁶¹ reported the presence of coumarin, *o*-coumaric acid and melilotic acid in leaf tissues of *Dipteryx odorata*, by extracting these constituents with HCl 20% v/v aqueous solution. Salicylic acid, ferulic acid and hydroxybenzoic acid, among others, were also identified by the author. Isoflavones were isolated from heartwood,

callus and roots using chloroform as solvent.^{62,63} Other flavonoids were identified in methanol extract from the bark⁶⁴ and heartwood⁶⁵ of the specie, and also in ethyl ether extract from the endocarp.⁶⁶

Concerning to cumaru seeds, Sullivan⁶⁷ reports the presence of umbelliferone (7-hydroxycoumarin) in methylene chloride extract. Jang *et al.*⁶⁸ isolated dipteryx acid, a cassane diterpene, and different subgroups of phenolic compounds from methanol extract of seeds collected in Peru. Oliveros-Bastidas *et al.*⁶⁹ report the presence of high fatty acid content in hexane extract of *Dipteryx odorata* (aubl.) Willd. seeds from Venezuelan regions. A polar extract (ethanol/water 1:1) from the same seeds sample contains 50% of 6,7-dihydroxycoumarin- β -D-glucopyranoside (esculin). The analysis also showed the presence of monomeric sugar and very low concentration of short chain carboxylic acid. The extraction of coumarin using ethanol as solvent and supercritical CO₂ was mentioned by Lima *et al.*⁷⁰

The aqueous extract of cumaru seeds prepared in this work was characterized by FTIR, ¹H, ¹³C and 2D NMR. The spectroscopic data point out the presence of carbohydrates and aromatic compounds with *ortho*-substitution profile. The analysis of the extract by Bradford method indicated the presence of low concentration of protein (0.11 mg mL⁻¹). This result is in consonance with the spectroscopic techniques, which not detected bands in FTIR spectrum and signals in NMR spectra characteristics of the presence of amino acids.

IR spectrum of the aqueous extract of cumaru seeds showed characteristic absorption bands of carbohydrates. A large band around 3472 cm⁻¹ corresponding to O–H bond and vibration of CH₂ and CH groups from sp³ carbons at 2925 and 2854 cm⁻¹, respectively, were observed. The presence of aromatic compounds in the extract is indicated by a low intensity band of C=C bond from aromatic ring (1655 cm⁻¹) and the C–H stretch of aromatic ring in 3008 cm⁻¹. A band at 1747 cm⁻¹ relative to C=O bond suggest the presence of carboxylic acids.

¹H and ¹³C NMR spectra showed characteristic signals of carbohydrates. In ¹H NMR spectrum, it was observed a signal at 5.4 ppm which can be attributed to anomeric proton. In ¹³C NMR spectrum, a signal at 92 ppm may be attributed to the anomeric carbon of free glucose in α -glycopyranoside form.⁷¹ The 2D heteronuclear single quantum coherence spectroscopy (HSQC) experiment showed a correlation between the signals at 5.4 and 92 ppm. The signal in 100 ppm (¹³C NMR spectrum) is also observed in positive phase of DEPT135 spectrum concluding that it belongs to a tertiary carbon (CH). Additionally, it correlates with a hydrogen that has 5.1 ppm chemical shift. It could be

associated to a polyhydroxylated ring such as a furanoside structure for example. The sp³ carbon signals between 70 and 82 ppm are relative to carbons bonded to hydroxyl groups (HC–OH). The signals between 60 and 62 ppm are assigned to primary carbons (CH₂OH). The assignments were confirmed by DEPT135 spectrum. In the HSQC spectrum, it is possible to observe the correlation between these carbon signals (from 60 to 82 ppm) with the hydrogen signals from 3.0 to 4.5 ppm, which are in agreement with carbon chain of carbohydrates (CH₂OH and HC–OH). The ¹³C NMR spectrum also showed a signal in 103.9 ppm which did not appear in DEPT135 spectrum, indicating that it belongs to a quaternary carbon. This data would be compatible, for example, with the presence of fructose. The chemical shifts observed in the NMR spectra are compatible, for example, with the polyhydroxylated compounds identified in the polar fraction of *Dipteryx odorata* seeds by Oliveros-Bastidas *et al.*⁶⁹

¹H and ¹³C NMR spectra also showed characteristic signals of aromatic compounds. The presence of coumarin in the extract is eliminated due to two observations in ¹³C NMR spectrum: (i) the absence of a signal at approximately 160 ppm, typical of a carbonyl carbon belonging to α,β -unsaturated lactone system; and (ii) the absence of a signal between 140 and 145 ppm, that would be assigned to carbon β . In ¹³C NMR spectrum, the presence of a carbonyl carbon signal was observed at 177 ppm, i.e., more deshielded than expected, being compatible with the presence of carboxylic group. The signals at 126.7 and 154 ppm were not observed in the DEPT135 spectrum, belonging to aromatic quaternary carbons. The chemical shift from the second carbon suggests it is connected to an oxygen atom. The DEPT135 spectrum showed six sp² carbon (CH) signals in 115, 123, 127, 128, 129.6 and 129.7 ppm. According to the 2D HSQC spectrum, all of them have correlation with hydrogens, whose signals were observed between 6 and 8 ppm. The analysis of the ¹H NMR spectrum shows that the signals of these hydrogens have unequivocal multiplicities. Four doublets are observed with chemical shifts centered on 6.1, 6.8, 7.1 and 7.4 ppm, and two triplets, on 7.0 and 7.3 ppm. All of them with the same integration value. These data are characteristic of an *ortho*-substituted aromatic ring. The doublets in 6.8 and 7.1 ppm have coupling constant of 10 Hz and both triplets of 7.5 Hz. The HSQC spectrum shows correlation between the signals 7.1 and 115 ppm, this carbon being next to the carbon bounded to oxygen. The doublets centered on 6.1 and 7.4 ppm are correlating with the carbon signals 128 and 129 ppm, respectively. The values indicate the presence of olefinic group, but they were not compatible with a coumaric acid structure.

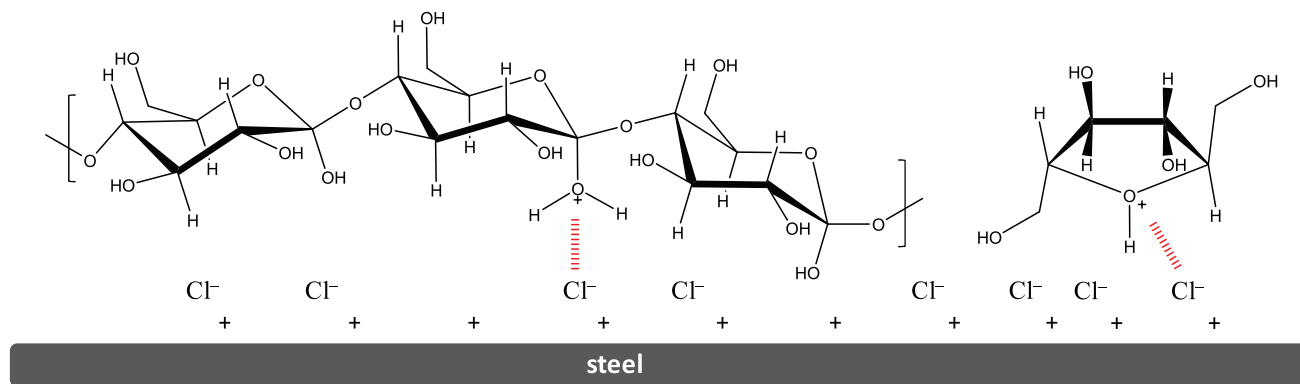


Figure 7. Simple representation of the inhibitory action by the electrostatic interaction of carbohydrates.

In the IR spectrum, the bands that indicate the presence of polyhydroxylated compounds predominate in comparison to the characteristic bands of aromatic compounds. In the ^1H and ^{13}C NMR spectra, the signals of carbons and hydrogens belonging to HC-OH and CH_2OH groups are more abundant and intense than the signals related to aromatic compounds. All analyzed spectra point to the majority presence of carbohydrates which could be responsible for the inhibitory action of the aqueous extract of cumaru seeds and its HMWF.

Inhibitory action mechanism

The chemical characterization of the dry extract of cumaru seeds showed that carbohydrates are the major compounds of the extract. Additionally, its HMWF presented higher IE than the total extract. This data indicated that the polysaccharide molecules are probably responsible for the inhibitory action.

The decrease in IE as temperature increases and the increase of the activation energy for the tests in the presence of both aqueous extract of cumaru seeds and its HMWF, evidenced a process of physical adsorption of the constituent molecules on the metallic surface. Based on this result, it is possible to propose that the anions present (in this case, chloride ions) were first adsorbed onto the metal surface making it negatively charged, and then the protonated inhibitory molecules (in this case, the protonated polysaccharides) are electrostatically adsorbed on the steel surface.³² If the metal surface is positively charged with respect to the potential of zero charge (PZC), the chloride ions will first be adsorbed on the metal surface, which attracts the protonated inhibitor molecules and protonated water molecules.⁷² This result could also explain the negative value of the lateral parameter of interaction between the adsorbed molecules (a), obtained from the adjustment of experimental data to Temkin's isotherm (Table 6). It suggests a repulsive force between the adsorbed

molecules, i.e., between the protonated polysaccharides molecules. Some computational studies^{73,74} have shown that in aqueous acidic medium, the chemical structure of this class of compounds can be protonated in the ring oxygen, as well as in hydroxyl groups bonded to specific carbons. Figure 7 shows a simplified representation of the inhibitory action by the carbohydrates.

Conclusions

The following conclusions can be drawn from this work.

(i) The aqueous extract of cumaru seeds and its high molecular weight fraction prevent the corrosion of mild steel in 1 mol L^{-1} HCl solution. The inhibition effect is concentration-dependent. The higher the concentration of inhibitor in the acid solution, the greater the efficiency of inhibition.

(ii) The exact chemical composition of the aqueous extract of cumaru seeds is not known. Even so, it is possible to assume that the inhibition efficiency observed in the results of weight-loss measurements and electrochemical experiments is promoted by the high molecular weight molecules present in the extract, since this fraction showed much more promising results.

(iii) The corrosion inhibition was significantly influenced by the immersion time. Even at low concentration, both aqueous extract of cumaru seeds and its high molecular weight fraction achieved high inhibition efficiency in longer immersion times.

(iv) The inhibition efficiency decreased as the temperature of the acid solution increased, suggesting the occurrence of physical adsorption of the compounds present in the aqueous extract of cumaru seeds in the mild steel surface. The apparent activation energy of mild steel in the HCl solution increased with the addition of both inhibitors, also indicating that they act through physical adsorption.

(v) The impedance spectroscopy shows only one capacitive loop even in the presence of the both inhibitors

which is attributed to the charge transfer and the double layer capacitance in the corrosive process. The presence of the dry extract and its HMWF changed the double electrical layer capacitance which may be caused by reduction in the local dielectric constant and/or by an increase in the thickness of the electrical double-layer. These results show that the presence of both inhibitors modifies the electric double-layer structure.

(vi) The results of potentiodynamic polarization measurements indicate that both the aqueous extract of cumaru seeds and its high molecular weight fraction behave as a mixed-type inhibitors, affecting both cathodic hydrogen evolution and anodic mild steel dissolution reactions.

(vii) The surface analysis showed that the aqueous extract of cumaru seeds as well as its high molecular weight fraction acts as good corrosion inhibitor, leaving the metal surface less rough, inhibiting the corrosive process. A thick film was observed with HMWF addition.

(viii) Based on the results of the high molecular weight fraction, it is possible to propose that macromolecules (probably polysaccharides) could be responsible for the inhibitory action observed by the aqueous extract of cumaru seeds.

Supplementary Information

Supplementary information (spectra of the characterization of the aqueous extract of cumaru seeds and Bode diagrams) associated with this article can be found available free of charge at <http://jbcbs.sbq.org.br> as PDF file.

Acknowledgments

The authors thank CNPq (Conselho Nacional de Desenvolvimento Científico e Tecnológico) for financial support (process numbers 424306/2016-6 and 421590/2016-5). The authors are also thankful to CNPq for the research fellowship for V. M. Teixeira.

Author Contributions

Viviane M. Teixeira was responsible for formal analysis, investigation, methodology, writing-original draft; Gustavo A. de Oliveira for investigation, methodology; Michelle J. C. Rezende for formal analysis, investigation, methodology, writing-original draft, writing-review and editing; Eliane D'Elia for conceptualization, formal analysis, funding acquisition, investigation, methodology, project administration, supervision, writing-original draft, writing-review and editing.

References

- Silva, M. V. F.; Pereira, M. C.; Codaro, E. M.; Acciari, H. A.; *Quim. Nova* **2015**, *38*, 293.
- Raja, P. B.; Sethuraman, M. G.; *Mater. Lett.* **2008**, *62*, 1602.
- Assunção, S. S.; Pêgas, M. M.; Fernandez, T. L.; Magalhães, M.; Schöntag, T. G.; Lago, D. C. B.; Senna, L.; D'Elia, E.; *Corros. Sci.* **2012**, *65*, 360.
- Ribeiro, K.; Cordeiro, R. F. B.; Orofino, H.; Nunes, J. C.; Magalhães, M.; Torres, A. G.; D'Elia, E.; *Int. J. Electrochem. Sci.* **2016**, *11*, 406.
- Oguzie, E. E.; *Corros. Sci.* **2008**, *50*, 2993.
- Bentrah, H.; Rahali, Y.; Chala, A.; *Corros. Sci.* **2014**, *82*, 426.
- Mainer, F. B.; Silva, R. R. C. M.; *Engvista* **2004**, *6*, 106.
- <http://periodicos.unisanta.br/index.php/sat/article/download/132/118>, accessed in September 2020.
- Resende, C.; Diniz, A. F.; Martelli, P. B.; Bueno, A. H. S.; *Rev. Virtual Quim.* **2017**, *9*, 699.
- Lashgari, M.; Arshadi, M. R.; Bigiar, M.; *Chem. Eng. Commun.* **2010**, *197*, 1303.
- Quraishi, M. A.; Sharma, H. K.; *Mater. Chem. Phys.* **2002**, *78*, 18.
- Saha, S. K.; Banerjee, P.; *RSC Adv.* **2015**, *87*, 71120.
- Li, W.; He, Q.; Pei, C.; Hou, B.; *Electrochim. Acta* **2007**, *52*, 6386.
- Abouchane, M.; El-Bakri, M.; Touir, R.; Rochdi, A.; Elkhatabi, O.; Touhami, M. E.; Forssal, I.; Mernari, B.; *Res. Chem. Intermed.* **2015**, *41*, 1907.
- Singh, P.; Quraishi, M. A.; *Measurement* **2016**, *86*, 114.
- Raja, P. B.; Sethuraman, M. G.; *Mater. Lett.* **2008**, *62*, 113.
- Torres, V. V.; Cabral, G. B.; da Silva, A. C. G.; Ferreira, K. C. R.; D'Elia, E.; *Quim. Nova* **2016**, *39*, 423.
- Rocha, J. C.; Gomes, J. A. A. P.; D'Elia, E.; Gil, A. P. C.; Cabral, L. M. C.; Torres, A. G.; Monteiro, M. V. C.; *Int. J. Electrochem. Sci.* **2012**, *7*, 11941.
- Rocha, J. C.; Gomes, J. A. A. P.; D'Elia, E.; *Mater. Res.* **2014**, *17*, 1581.
- Rocha, J. C.; Gomes, J. A. A. P.; D'Elia, E.; *Corros. Sci.* **2010**, *52*, 2341.
- Paul, S.; Kar, B.; *ISRN Corros.* **2012**, ID 641386.
- Gunasekaran, G.; Chongdar, S.; Gaonkar, S. N.; Kumar, P.; *Corros. Sci.* **2004**, *46*, 1953.
- Abboud, Y.; Tanane, O.; El Bouari, A.; Salghi, R.; Hammouti, B.; Chetouani, A.; Jodeh, S.; *Corros. Eng., Sci. Technol.* **2016**, *5*, 557.
- Akalezi, C. O.; Ogukwe, C. E.; Ejele, E. A.; Oguzie, E. E.; *Int. J. Corros. Scale Inhib.* **2016**, *5*, 132.
- Patni, N.; Agarwal, S.; Shah, P.; *Chin. J. Eng.* **2013**, ID 784186.
- Trindade, R. S.; Santos, M. R.; Cordeiro, R. F. B.; D'Elia, E.; *Green Chem. Lett. Rev.* **2017**, *10*, 444.
- Zau, M. D. L.; Vasconcelos, R. P.; Giaccon, V. M.; Lahr, F. A. R.; *Polim.: Cienc. Tecnol.* **2014**, *24*, 726.

28. <https://www.infoteca.cnptia.embrapa.br/infoteca/bitstream/doc/5786571/1/CT225.pdf>, accessed in September 2020.
29. Felix, R. A. Z.; Ono, E. O.; Silva, C. P.; Rodriguez, J. D.; Perre, C.; *Rev. Bras. Biocienc.* **2007**, *5*, 138.
30. <http://www.cumaruamazonia.com.br/>, accessed in September 2020.
31. Teixeira, V. M.; Santos, E. C.; Rezende, M. J. C.; D'Elia, E.; *Rev. Virtual Quim.* **2015**, *7*, 1780.
32. Rodrigues, L. S.; Valle, A. F.; D'Elia, E.; *Int. J. Electrochem. Sci.* **2018**, *13*, 6169.
33. Cordeiro, R. F. B.; Belati, A. J. S.; Perrone, D.; D'Elia, E.; *Int. J. Electrochem. Sci.* **2018**, *13*, 12188.
34. Santos, E. C.; Cordeiro, R. F. B.; Santos, M.; Rodrigues, P. R. P.; Singh, A.; D'Elia, E.; *Mater. Res.* **2019**, *22*, e20180511.
35. Santana, C. A.; da Cunha, J. N.; Rodrigues, J. G. A.; Greco-Duarte, J.; Freire, D. M. G.; D'Elia, E.; *J. Braz. Chem. Soc.* **2020**, *31*, 1225.
36. ASTM G31-7: *Standard Guide for Laboratory Immersion Corrosion Testing of Metals*, West Conshohocken, 2013.
37. Muthukrishnan, P.; Prakash, P.; Jeyaprabha, B.; Shankar, K.; *Arabian J. Chem.* **2015**, *12*, 3345.
38. Singh, A.; Ebenso, E. E.; *Int. J. Electrochem. Sci.* **2013**, *8*, 12874.
39. Yaro, A. S.; Khadom, A. A.; Wael, R. K.; *Alexandria Eng. J.* **2013**, *52*, 129.
40. Singh, A.; Ahamad, I.; Singh, V. K.; Quraishi, M. A.; *J. Solid State Electrochem.* **2011**, *15*, 1087.
41. Deyab, M. A.; El-Rehim, S. S. A.; *Int. J. Electrochem. Sci.* **2013**, *8*, 12613.
42. Szauer, T.; Brandt, A.; *Electrochim. Acta* **1981**, *26*, 1209.
43. Kuznetsov, Y. I.; Andreev, N. N.; Vesely, S. S.; *Int. J. Corros. Scale Inhib.* **2015**, *4*, 108.
44. Fernandes, C. M.; Fagundes, T. S. F.; Santos, N. E.; Rocha, T. S. M.; Garret, R.; Borges, R. M.; Muricy, G.; Valverde, A. L.; Ponzio, E. A.; *Electrochim. Acta* **2019**, *312*, 137.
45. Umoren, S. A.; Gasem, Z. M.; Obot, I. B.; *Ind. Eng. Chem. Res.* **2013**, *52*, 14855.
46. Bentiss, F.; Lebrini, M.; Lagrene'e, M.; *Corros. Sci.* **2005**, *47*, 2915.
47. Zhang, Z.; Tian, N.; Zhang, W.; Huang X.; Ruan, L.; Wu, L.; *Corros. Sci.* **2016**, *111*, 675.
48. Mourya, P.; Banerjee, S.; Singh, M. M.; *Corros. Sci.* **2014**, *85*, 352.
49. Souza, T. F.; Magalhães, M.; Torres, V. V.; D'Elia, E.; *Int. J. Electrochem. Sci.* **2015**, *10*, 22.
50. El-Awady, A. A.; Abd-El-Nabey, B. A.; Aziz, S. G.; *J. Electrochem. Soc.* **1992**, *139*, 2149.
51. Karthikaiselvi, R.; Subhashini, S.; *J. Assoc. Arab Univ. Basic Appl. Sci.* **2014**, *16*, 74.
52. Dotto, G. L.; Vieira, M. L. G.; Gonçalves, J. O.; Pinto, L. A. A.; *Quim. Nova* **2011**, *34*, 1193.
53. Moura, E. C. M.; Souza, A. D. N.; Rossi, C. G. F. T.; Silva, D. R.; Maciel, M. A. M. M.; *Quim. Nova* **2013**, *36*, 59.
54. Aoki, I. V.; Guedes, I. C.; *J. Appl. Electrochem.* **2002**, *32*, 915.
55. de Souza, F. S.; Gonçalves, R. S.; Spinelli, A.; *J. Braz. Chem. Soc.* **2014**, *25*, 81.
56. Souza, E. C. C. A.; Ripper, B. A.; Perrone, D.; D'Elia, E.; *Mater. Res.* **2016**, *19*, 1276.
57. Yurt, A.; Balaban, S.; Kandemir, U.; Bereket, G.; Erk, B.; *Mater. Chem. Phys.* **2004**, *85*, 420.
58. Tebbji, K.; Hammouti, B.; Oudda, H.; Ramdani, A.; Benkadour, M.; *Appl. Surf. Sci.* **2005**, *252*, 1378.
59. Morad, M. S.; El-Dean, A. M. K.; *Corros. Sci.* **2006**, *48*, 3398.
60. Verma, C.; Quraishi, M. A.; Singh, A.; *J. Mol. Liq.* **2015**, *212*, 804.
61. Griffiths, L. A.; *J. Exp. Bot.* **1962**, *13*, 169.
62. Hayashi, T.; Thomson, R. H.; *Phytochemistry* **1974**, *13*, 1943.
63. Januário, A. H.; Lourenço, M. V.; Domézio, L. A.; Pietro, R. C. L. R.; Castilho, M. S.; Tomazela, D. M.; Silva, M. F. G. F.; Vieira, P. C.; Fernandes, J. B.; França, S. C.; *Chem. Pharm. Bull.* **2005**, *53*, 740.
64. Nakano, T.; Alonso, J.; Grillet, R.; Martin, A.; *J. Chem. Soc., Perkin Trans. 1* **1979**, *1*, 2107.
65. Imai, T.; Inoue, S.; Ohdaira, N.; Matsushita, Y.; Suzuki, R.; Sakurai, M.; Jesus, J. M. H.; Ozaki, S. K.; Finger, Z.; Fukushima, K.; *Wood Sci.* **2008**, *54*, 470.
66. Cunha, C. P.; Godoy, R. L. O.; Braz-Filho, R.; *Rev. Virtual Quim.* **2016**, *8*, 43.
67. Sullivan, G.; *J. Agric. Food Chem.* **1982**, *30*, 609.
68. Jang, D. S.; Park, E. J.; Hawthorne, M. E.; Vigo, J. S.; Graham, J. G.; Cabieses, F.; Santarsiero, B. D.; Mesecar, A. D.; Fong, H. H. S.; Mehta, R. G.; Pezzuto, J. M.; Kinghorn, A. D.; *J. Nat. Prod.* **2003**, *66*, 583.
69. Oliveros-Bastidas, A. J.; Demuner, A. J.; Barbosa, L. C. A.; *Quim. Nova* **2013**, *36*, 502.
70. Lima, J. C.; Traczynski, M.; Giufrida, W. M.; Feihmann, A. C.; Freitas, L. S.; Cardozo-Filho, L.; *Chem. Eng. Trans.* **2017**, *57*, 1801.
71. Pretsch, E.; Bühlmann, P.; Badertscher, M.; *Structure Determination of Organic Compounds-Tables of Spectral Data*; SpringerVerlag: Berlin Heidelberg, 2009, ch. 4, p. 148.
72. Vinutha, M. R.; Venkatesha, T. V.; *Port. Electrochim. Acta* **2016**, *34*, 157.
73. Yang, G.; Pidko, E. A.; Hensen, E. J. M.; *J. Catal.* **2012**, *295*, 122.
74. Kennedy, J.; Wu, J.; Drew, K.; Carmichael, I.; Serianni, A. S.; *J. Am. Chem. Soc.* **1997**, *119*, 8933.

Submitted: May 12, 2020

Published online: September 28, 2020

